Portable Instrument for Online Investigations of Optical Properties of Airborne Particles

Julian Robertz*, Aleksandar Duric, Martin Allemann
Siemens Schweiz AG, Building Technologies Division, Zug, Switzerland

Daniel Egli, Markus Loepfe, Heinz Burtscher
University of Applied Sciences and Arts Northwestern Switzerland, Windisch, Switzerland

Hans-Joachim Schöpe
University of Tübingen, Institute of Applied Physics, Tübingen, Germany

**Also affiliated with the University of Tübingen*

Abstract

For the development of photoelectric fire detectors the discrimination of smoke from nuisance aerosols is still one of the main goals. In order to improve our understanding of optical properties of airborne particles and to determine different quantities like morphology, refractive index or size distribution, a time resolved online measurement instrument is highly advantageous.

The presented instrument measures fourteen scattering vectors at two wavelengths and two different polarization directions of the incident light. Main effort was put on achieving high stability and high dynamic range by carefully designing the optics and exploiting a wide measurement range of the detectors. As a result the dynamic range is improved by approximately a factor of three (compared to [1]). The time resolution has been increased by a factor of two although the number of measured polarization states has been doubled.

A fast and field-capable calibration method was developed, enabling for a quick set-up in the field, while keeping the accuracy as close as possible to the laboratory conditions. Scattered light and particle size distribution measurements with Di-Ethyl-Hexyl-Sebacat (DEHS) aerosol were performed and compared to Mie scattering calculations in order to verify the calibration.

As a next step a comprehensive data base of aerosol optical properties including polarization dependent scattering will be collected serving as a basis for designing novel fire detectors.

Keywords: light scattering, dynamic range, optical design, polarization, calibration, online measurements

Introduction

Creating a scattered-light fire-detection technology being capable of distinguishing smoke from nuisance aerosols with high reliability requires an in-depth understanding of their optical properties. This information needs to be combined with understanding of dynamics and temporal evolution of fires. Therefore the multi-angle, dual-wavelength scattering chamber [1] presented on AUBE'14 was improved and new functions, like changing of the polarization state of the incident light and measurement of the laser power after passing the chamber, were added.

Increasing the dynamic range

A large dynamic range of the instrument is required because of the high intensity variation of the scattered light and a typical temporal development of fires. One goal was to reduce the background scattering within the chamber. This was achieved by using collimated laser beams and laminating the chamber with a ultra-black coated foil. As a result the background scattering was reduced to below 1 % of the dynamic range of the detectors while using typical laser powers.

Homogenous illumination of the scattering volume and a minimum background scattering can be reached by propagating a laser beam with a fundamental transverse Gaussian mode (TEM_{00}). This was achieved by using single-mode fibers between the laser heads and the scattering chamber.

The propagation of a TEM_{00}-mode through the scattering chamber can be easily calculated with the ray transfer matrix analysis [2] under the assumption of ideal optical elements. The start properties are given by the fiber specifications and the end of the fiber at the position (0,0) (Fig. 1). The diameter of the collimated laser beam was set to be around $d_l \approx 1\ \mathrm{mm}$ having a diameter of the aerosol stream of $d_a \cong 0.7\ \mathrm{mm}$. The determined beam diameters are plotted in the chamber cross section (Fig. 1). Another design criterion was the limitation of the stray light (higher modes) to less than 1 % of the power. Therefore the beam radius times 2.3 (dashed line in Fig. 1) is not allowed to collide with the chamber elements [3].

In order to avoid damages to the optical elements the maximum allowable power limited by the laser-induced damage threshold (LIDT) of the optics was estimated according to [4]. The linear polarizers, having the minimum LIDT of the applied optical components, limit the allowable laser powers to $P_{405\mathrm{nm}} = 50\ \mathrm{mW}$ and $P_{852\mathrm{nm}} = 20\ \mathrm{mW}$. These polarizers remove the remaining cross polarization after the polarization maintaining (PM) fibers. Such fibers are necessary because otherwise small mechanical deformations of the fibers modify the polarization states and lead to large power fluctuations after the polarizers.

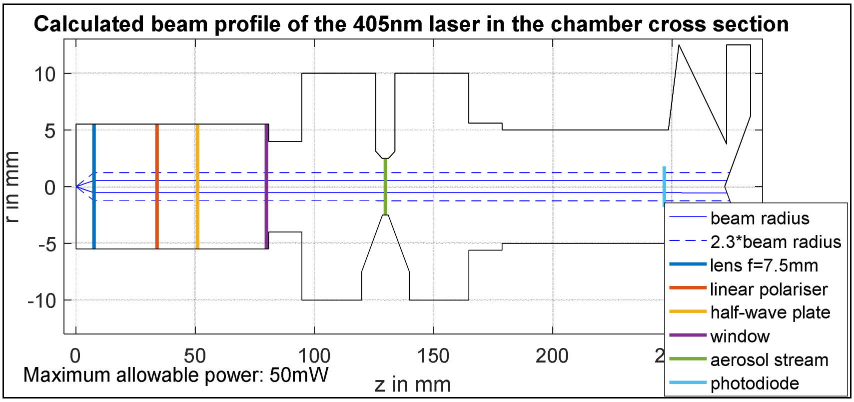

Fig. 1. Calculated beam profile of the 405 nm laser transformed by the optical elements.

The beam properties were determined by partially blocking the beam in vertical and horizontal direction with a moving knife edge and measuring the remaining intensity. The results are $d_{l,405\text{nm}} = 1.03\text{ mm}$ and $d_{l,852\text{nm}} = 0.89\text{ mm}$ compared to calculated $d^{(\text{theo})}_{l,405\text{nm}} = 1.08\text{ mm}$ and $d^{(\text{theo})}_{l,852\text{nm}} = 1.03\text{ mm}$, respectively. Further improving could be achieved with special and more expensive collimators instead of plano-convex lenses.

The non-linear counting rate (see Fig. 2) of the multi pixel photon counters (MPPC) has to be corrected numerically, especially for high counting rates: Laser light can be approximated as a coherent state $|\alpha\rangle$ [5] which yields to a Poisson distribution for the incoming photons:

$$\mathcal{P}_{\bar{n}}(n) = \frac{\bar{n}^n}{n!}\mathrm{e}^{-\bar{n}}. \quad \text{(Eq. 1)}$$

$\bar{n}$ is the average number of measured photons in a specific time and $\mathcal{P}_{\bar{n}}(n)$ the probability to measure n photons in that time. The used MPPCs can only count a new detection event after at least $\tau \approx 15\text{ ns}$ have passed since the last one. The average number of measured photons $\bar{n}$ per time t is given by the detection rate $\bar{d} = \bar{n}/t$. With that the probability to measure in the time τ zero photons results in $\mathcal{P}_{\bar{n}(\tau)}(0)$ and finally in the average counting rate [8]

$$\bar{c}(\tau, \bar{d}) = \bar{d}\mathcal{P}_{\bar{n}(\tau)}(0) = \bar{d}\mathrm{e}^{-\tau\bar{d}}. \quad \text{(Eq. 2)}$$

In Fig. 2 a measurement of the counting rate depending on the detection rate shows good agreement with the theoretical curve (Eq. 2). Therefore it is feasible to calculate the detection rate of the measured counting rate. In order to ensure to measure always at the left side of the maximum of the curve $\bar{c} = 15 \cdot 10^6\text{ s}^{-1}$ was implemented as maximum allowable counting rate. Together with the reduced background the overall improvement of the dynamic range is approximately a factor of three compared to [1].

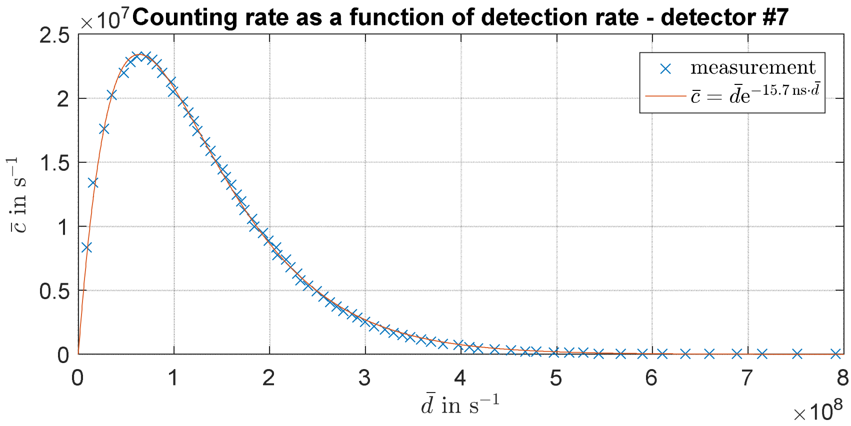

Fig. 2. Counting rate $\bar{c}$ as a function of the detection rate $\bar{d}$ of detector #7 with the fitted theoretical curve as in Eq. 2.

Changing the polarization state

The main new functionality compared to the setup presented in [1] is the possibility to change the polarization state of the incident laser light. For each laser beam a half-wave plate in a motorized rotator was placed in front of the chamber before the beam entrance (Fig. 3). By rotating the half-wave plate the polarization state of the incident light can be changed within approximately 250 ms from horizontal to vertical. Therefore both polarization directions and both wavelengths can be analyzed within one measuring cycle of 2.5 s. Other polarization angles of the incident light can be easily produced by changing the software parameters of the rotators.

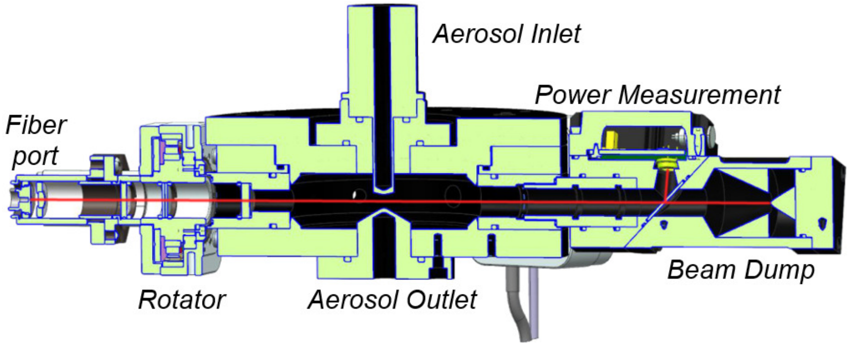

Fig. 3. Cross section of the scattering chamber with the laser beam represented as a red line.

The angles for the rotators were determined by measuring the minimum transmission through a crossed linear polarizer with a precision of $\Delta\varphi \leq 0.1°$. Accordingly the orthogonality of the two polarization states is accurate up to $\Delta(\phi_{\perp} - \phi_{\parallel}) \leq 0.4°$ and the polarization angle itself up to $\Delta\phi \leq 1°$. The measured polarization extinction ratios for both wavelengths $\mathrm{ER}_{405\mathrm{nm}} > 1{:}250$ and $\mathrm{ER}_{852\mathrm{nm}} > 1{:}1200$ were well above the specification of the used polarization analyzers.

In order to improve the accuracy of the measured light intensities the corresponding incident laser power has to be determined. This measurement is made in the beam dump after the beam passed the chamber (Fig. 3). In front of each beam dump a glass plate is positioned with 45° angle to the beam axis. The plate reflects about 3 % of the light towards a photodiode which measures the laser power. The reflectivity of the glass plate depends on the incoming polarization and therefore each laser and polarization state has to be calibrated individually. The achieved measurement accuracy of the laser power is $\Delta P_{405\mathrm{nm}} \leq 0.9$ % and $\Delta P_{852\mathrm{nm}} \leq 3.4$ %.

Calibration and polarimetric characterization

Rayleigh scattering describes scattering of electromagnetic radiation at particles with size a small compared to the wave vector $k = 2\pi/\lambda$ [6]. The differential scattering cross section is given by:

$$\frac{\mathrm{d}\sigma}{\mathrm{d}\Omega} = k^4 a^6 \left|\frac{m^2-1}{m^2+2}\right|^2 (1 - \sin^2\theta \cdot \cos^2\phi), \qquad \text{(Eq. 3)}$$

where m is the refractive index of the particle material relative to the surrounding medium, θ the scattering angle and ϕ the polarization angle. The expression $1 - \sin^2\theta \cdot \cos^2\phi$ reduces to 1 for vertical and to $\cos^2\theta$ for horizontal polarization.

We found a simple and accurate method for calibration at both polarization directions and both wavelengths of the incident light by exploiting light scattering on gas molecules [7]. The method is based on the fact that the angular distribution of the differential scattering cross section for Rayleigh scatterers is independent of their structure and size.

The measured scattering intensity values for horizontal polarization at $\lambda = 405$ nm and $\lambda = 852$ nm were divided by the $\cos^2\theta$ factors of the corresponding scattering angles. These $\cos^2$-adjusted values for horizontal polarization and the values for vertical polarization have now to be the same for all detectors at a given wavelength. Given that, for each detector-wavelength pair a calibration factor correcting the differences in the scattering volume and detection efficiencies can be calculated. In our implementation the weighted least square method was used for evaluating the factors. Separate factors for both polarization directions are not necessary, because the influence of the optical elements between the scattering volume and the detectors on the polarization state can be neglected.

The calibrated (corrected) measurement values are shown in Fig. 4. The error of the calibration factors for 405 nm is less than 0.7 %. The error for 852 nm is approximately 15 %, which is due to a very low signal to noise ratio, caused by the comparatively low available power of the infrared laser. Therefore the values at $\lambda = 852\,\mathrm{nm}$, $\theta = 83°$ and horizontal polarization couldn't be measured. The uncertainty of the calibration factors includes error propagation from laser power measurement and background signals [8].

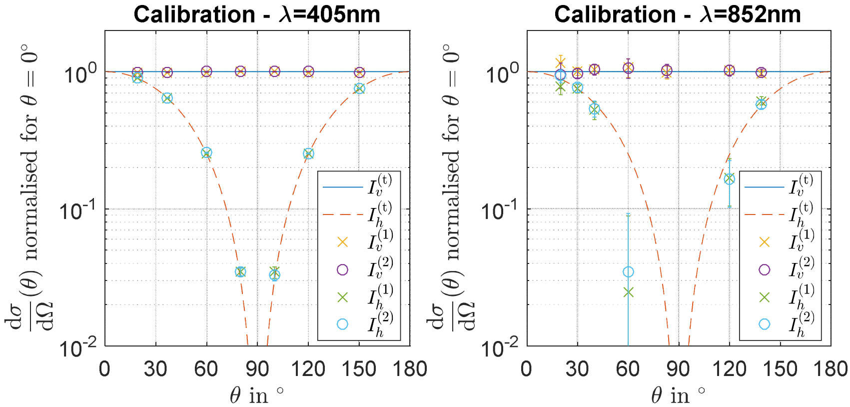

Fig. 4. Theoretical curves and the two measurements used for calibration with error bars denoting standard deviation.

The polarization misalignment $\Delta\phi$ contributes to the overall error of the scattered signals. For Rayleigh scattering it is less than 0.04 % for the vertical polarization. The error for horizontal polarization depends strongly on the scattering angle θ:

$$\frac{\Delta I_{\mathrm{scat}}(\theta)}{I_{\mathrm{scat}}} = \frac{1-\sin^2\theta \cdot \cos^2\Delta\phi}{\cos^2\theta} \quad \text{(Eq. 4)}$$

and approaches infinity for $\theta \to 90°$. For the measured scattering angles it is less than 2.1 %.

Measurement of particle size distribution

The calibration was verified by measuring Di-Ethyl-Hexyl-Sebacat (DEHS) aerosol. The DEHS particles were produced by an AGF 2.0 aerosol generator (Palas), which approximately show a lognormal size distribution. The aerosol size distribution was measured with a scanning mobility particle sizer (SMPS) resulting in a geometric mean diameter of 320 nm and geometric standard deviation of 1.85. For this distribution, the differential scattering coefficient was calculated by using Mie theory. For each geometric mean d_i of a distribution bin i, the differential scattering cross-section was calculated with a Matlab implementation of Bohren-Huffman Mie code [6, 9]. By multiplying it with the number of particles n_i within the corresponding bin i and summing up over all bins one obtains the differential scattering cross-section for the entire particle population:

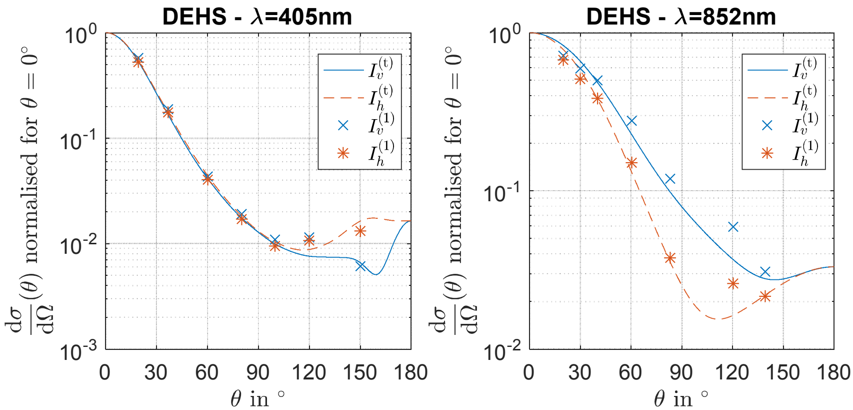

Fig. 5. Calculated relative scattering intensities for the measured particle size distribution compared to measured values.

$$\frac{d\sigma}{d\Omega}(\theta) = \sum_i n_i \frac{d\sigma}{d\Omega}(d_i, \theta). \quad \text{(Eq. 5)}$$

Normalized values for $\theta = 0°$ are shown in Fig. 5, solid lines. These values are compared to the experimental data, corrected by a constant scaling factor to match the calculated data.

An excellent agreement between the experimental and theoretical values for both vertical and horizontal polarisation is obtained for 405 nm (Fig 5, left hand-side). For 852 nm the deviation from the theoretical values is higher than for 405 nm. This can be partly attributed to the calibration uncertainty for the 852 nm channel due to the limited available laser power. However, the deviation at 120° is higher than expected from the calibration uncertainty. This requires further investigation.

Conclusions

The here presented instrument measures fourteen scattering vectors at two wavelengths and two different polarization directions of the incident light. Compared to the previous version of the instrument [1], the number of measured polarization states has been doubled and the optics were redesigned for significantly lower background signals. The measurement range of the detectors was also extended, resulting in an overall dynamic range improvement by approximately a factor of three. The time resolution of single measurements has been increased by a factor of two by software improvements.

A calibration method based on Rayleigh scattering on large gas molecules was developed. The calibration accuracy for 405 nm and 852 nm channels was determined to be 0.7 % and 15 %, respectively, for both polarization states.

The calibration and the polarization properties of the instrument were verified by measuring a Di-Ethyl-Hexyl-Sebacat (DEHS) aerosol with a rather broad particle size distribution and comparing the measurement with the Mie scattering theory. For 405 nm an excellent agreement was obtained, whereas for 852 nm the deviation is higher.

As a next step measurement campaigns with fire and non-fire aerosols are planned. A data base of aerosol optical properties including polarisation dependent scattering will be collected. A set of scattering angles and polarization states providing optimum differentiation of fires and nuisances will be derived.

References

[1] Z. Jurányi, et al, "*Application of the Rayleigh-Debye-Gans theory on the scattering of light by standard test fire aerosols*", 15th International Conference on Automatic Fire Detection, Duisburg, Germany, October 14-16, 2014.

[2] D. Meschede, "*Optik, Licht und Laser; 3., durchgesehene Auflage*", Vieweg + Teubner, Wiesbaden, Germany, 2008.

[3] N. Kämpfer, "Optik im Millimeter- und Submillimeterbereich", University of Bern, Institute of Applied Physics, Bern, Switzerland, 2004.

[4] "*Damage Thresholds*" and "*LIDT Calculations*", www.thorlabs.de/newgrouppage9.cfm?objectgroup_id=9025, Thorlabs Inc, Newton, United States, accessed on 09.09.2016.

[5] M. Fox, "*Quantum Optics: An Introduction. Oxford Master Series in Physics*", Oxford University Press, New York, United States, 2006.

[6] C.F. Bohren, D.R. Huffman, "*Absorption and Scattering of Light by Small Particles*", John Wiley & Sons, Inc, New York, United States, 1983.

[7] S. Zadoo, J.E. Thompson, "*Rayleigh scattering measurements of several fluorocarbon gases*", Journal of Environmental Monitoring, 2011.

[8] H. Pruys, "*Datenanalyse*", University of Zürich, Institute of Physics, Zürich, Switzerland, 2004.

[9] C. Mätzler, "*MATLAB Mie Scattering with and without Diffraction*", http://www.iap.unibe.ch/publications/pub-detail.php?lang=en&id=835, University of Bern, Institute of Applied Physics, Bern, Switzerland, 2004, accessed on 22.10.2014.